Supporting Information

Molecular DNA Dendron Vaccines

Max E. Distler[a,b,1], John P. Cavaliere[a,b,1], Michelle H. Teplensky[a,b], Michael Evangelopoulos[b,c], and Chad A. Mirkin[a,b,c,2], chadnano@northwestern.edu

[a]Department of Chemistry, Northwestern University, Evanston, IL 60208

[b]International Institute for Nanotechnology, Northwestern University, Evanston, IL 60208

[c]Department of Biomedical Engineering, Northwestern University, Evanston, IL 60208

[2]To whom correspondence may be addressed. Email: chadnano@northwestern.edu.

Contributed by Chad A. Mirkin; received September 2, 2022; accepted December 12, 2022; reviewed by David J. Mooney and Nicole F. Steinmetz

Author contributions: Conceptualization, M.E.D.; Methodology, M.E.D., J.P.C., M.H.T.; Validation, M.E.D. and J.P.C.; Formal analysis, M.E.D. Investigation, M.E.D., J.P.C., M.H.T, M.E, C.A.M.; Data curation, M.E.D.; Writing – original draft, M.E.D.; Writing – review and editing, M.E.D., J.P.C., M.H.T., M.E., C.A.M.; Visualization, M.E.D. and M.H.T. Supervision, C.A.M.

[1]M.E.D. and J.P.C. contributed equally to this work.

Table of Contents

DNA Design and Characterization

Table S1. DNA Design

Name	DNA Sequence (5' - 3')	Calc'd MW	Exp't MW
1826 CpG	TCC ATG ACG TTC CTG ACG TT	6059	6057
Dn1a	TTT TTT TTT T D Tr Sp Cy3 TCC ATG ACG TTC CTG ACG TT	26643.94	26701
Dn1aH	TTT TTT TTT T D Tr Sp Cy3 AAC GTC AGG AAC GTC ATG GA	26760.04	26767
Dn6a	TCC ATG ACG TTC CTG ACG TT D Tr Sp Cy3 TTT TTT TTT T	42038.84	42015
Dn6aH	AAC GTC AGG AAC GTC ATG GA D Tr Sp Cy3 TTT TTT TTT T	42735.44	42775
Dn1	TTT TTT TTT T D Tr Sp Cy3 TCC ATG ACG TTC CTG ACG T AmdT	26798.14	26803
Dn6m	TTT TT AmdT TTT T D Tr Sp Cy3 TCC ATG ACG TTC CTG ACG TT	27569.24	27588
Dn6e	AmdT TTT TTT TTT D Tr Sp Cy3 TCC ATG ACG TTC CTG ACG TT	27569.24	27553

Acronyms for phosphoramidites:

Sp: 18-O-Dimethoxytritylhexaethyleneglycol,1-[(2-cyanoethyl)-(N,N-diisopropyl)]-phosphoramidite (Spacer phosphoramidite 18)

D: 1,3-bis-[5-(4,4'-dimethoxytrityloxy)pentylamido]propyl-2-[(2-cyanoethyl)-(N,N-diisopropyl)]phosphoramidite (Symmetric doubler phosphoramidite)

Tr: Tris-2,2,2-[3-(4,4'-dimethoxytrityloxy)propyloxymethyl]methyleneoxypropyl-[(2-cyanoethyl)-(N,Ndiisopropyl)]-phosphoramidite (Long trebler phosphoramidite)

Cy3: 1-[3-(4-monomethoxytrityloxy)propyl]-1'-[3-[(2-cyanoethyl)-(N,N-diisopropyl) phosphoramidityl]propyl]-3,3,3',3'-tetramethylindocarbocyanine chloride (Cyanine 3 phosphoramidite)

AmdT: 5'-Dimethoxytrityl-5-[N-(trifluoroacetylaminohexyl)-3-acrylimido]-2'-deoxyUridine,3'-[(2-cyanoethyl)-(N,N-diisopropyl)]-phosphoramidite (Amino Modifier C6 dT)

Peptide Sequence Information

Table S2. Peptide Sequence

Name	Amino Acid Sequence (N - C)	MW
$E6^{49–58}$ (V10C)	VYDFAFRDLC	1248

Peptides were obtained through GenScript at ≥95% purity.

DNA Dendron Additional Characterization

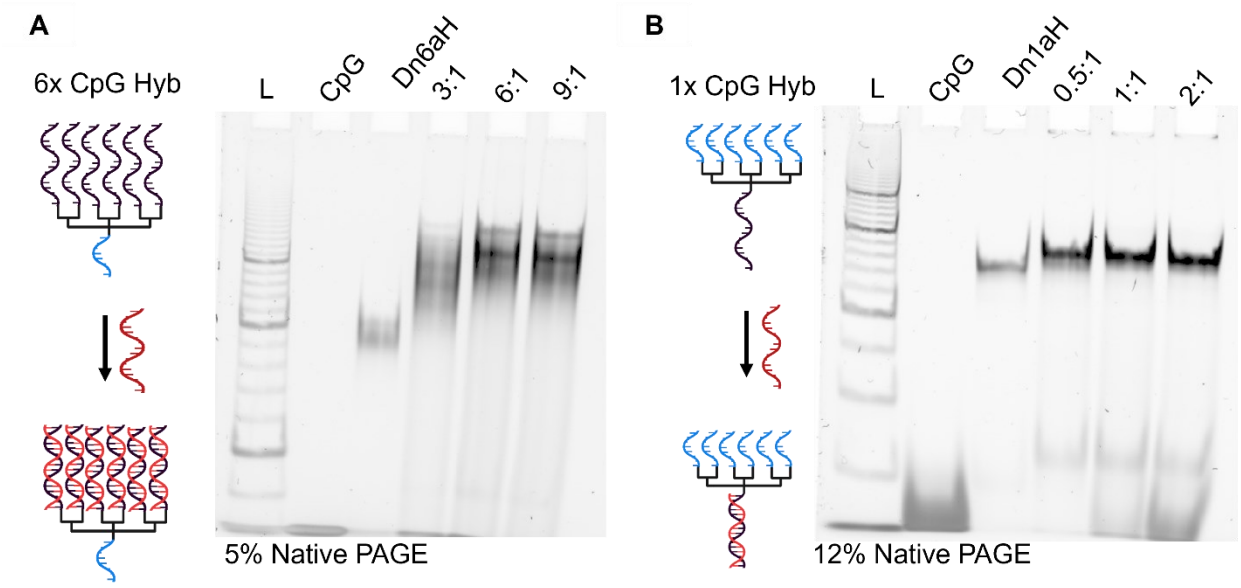

Figure S1. Hybridized dendron designs, Dn1aH and Dn6aH, were formed by combining the DNA dendrons with the CpG strands at stoichiometric amounts and annealing from 90-20 °C over 1 h. By tuning the relative amount of CpG added, we determined that a 1:1 ratio of CpG complement to CpG strand can be used to form the full hybridized structures Dn6aH (left) and Dn1aH (right).

DNA Dendron Uptake with Increasing Branch Length

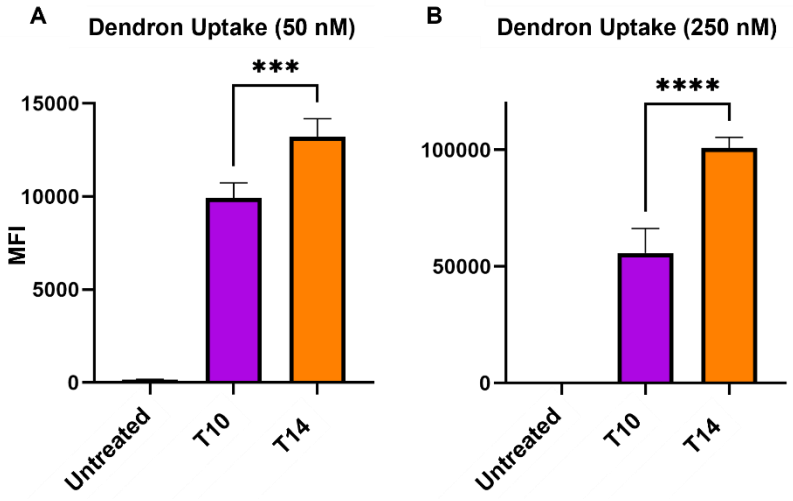

Figure S2. Dendron uptake with increasing branch length. Cells were treated with DNA dendrons that contained either T10 branches or T14 branches. We observe that longer branches result in increased cellular uptake at treatment concentrations of 50 and 250 nM.

Frequency of Costimulatory Marker Expression in Dendritic Cells

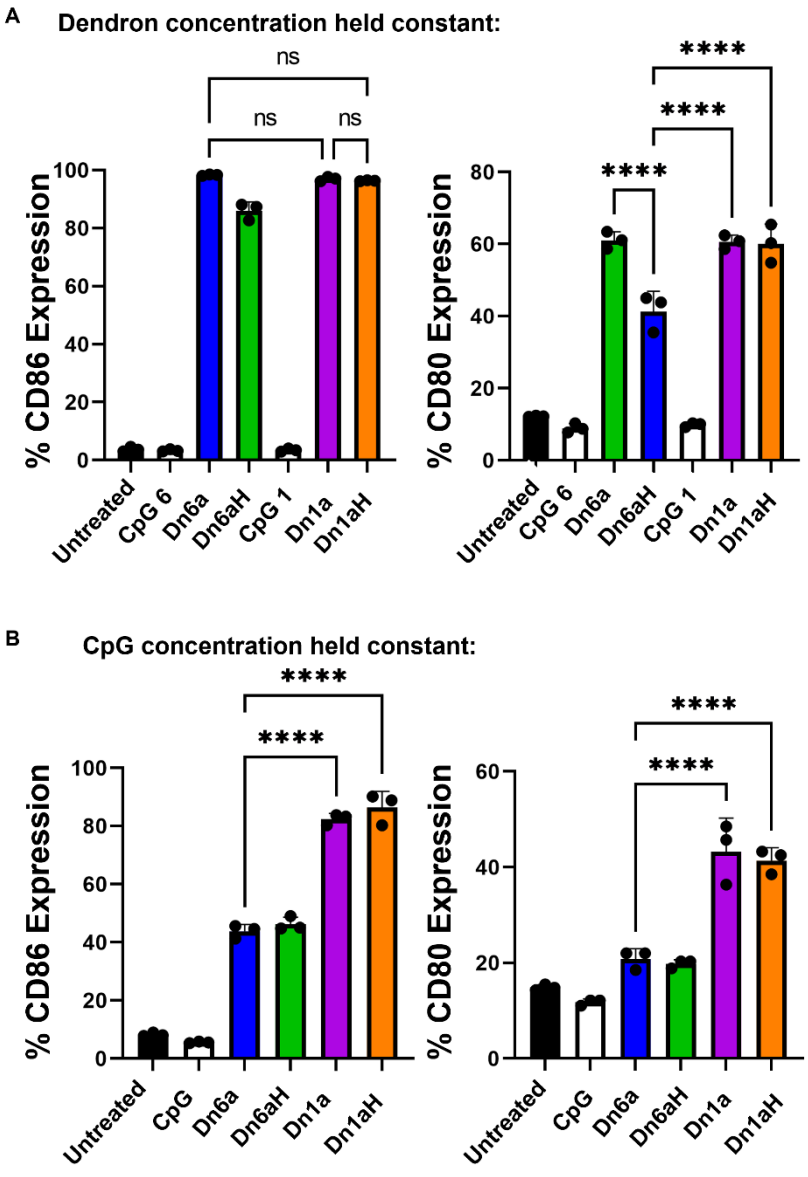

Figure S3. Frequency of cells expressing CD86 and CD80 in response to treatment with the different dendron designs. These trends match what is observed for the amount of CD86 and CD80 expression, with the greatest differences arising when CpG concentration is held constant.

Branch Sequence Effects on Dendritic Cell Uptake and Activation

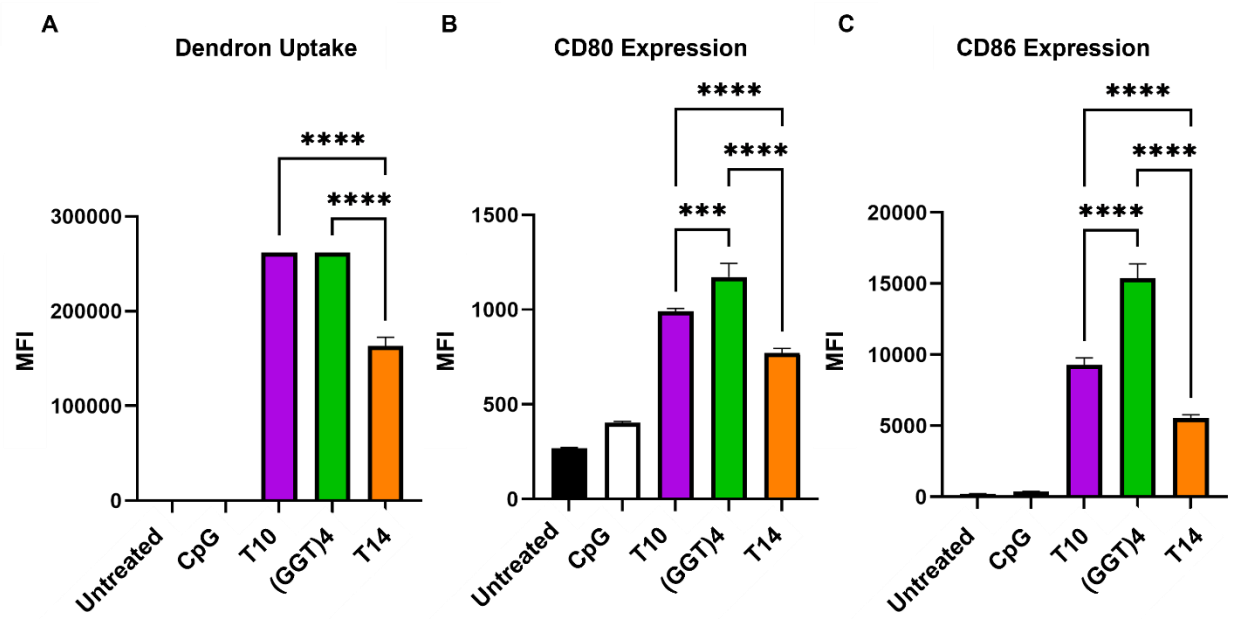

Figure S4. Dendritic cells were treated with either a CpG linear control, Dn1a with T10 branches, Dn1a with G-rich branches ((GGT)4), or Dn1a with T14 branches, which match the G-rich sequence in terms of the number of bases. After 15 h, we observe that the G-rich branches have comparable uptake to the T10 branches, but results in a significant increase in DC activation (CD80 and CD86 expression).

Effects of Primary Amines at Different Locations in the Dendron Structure

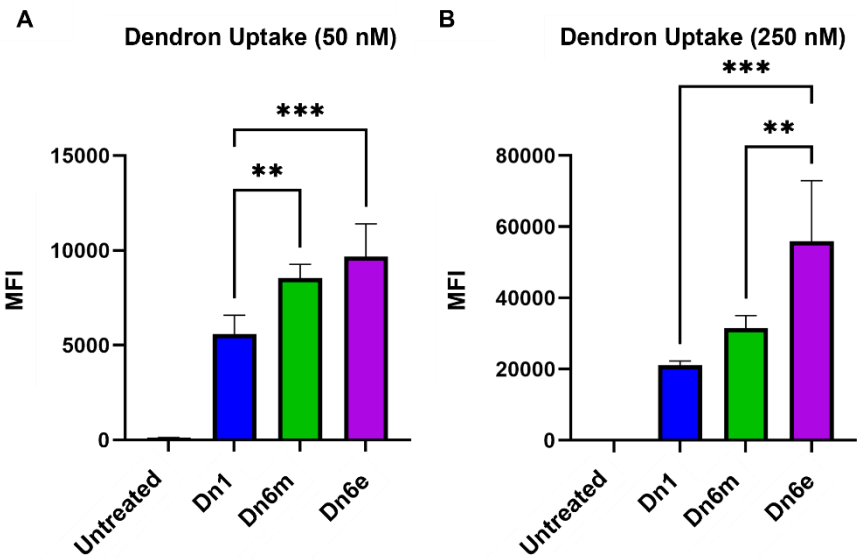

Figure S5. Dn1, Dn6m, and Dn6e are the dendrons that contain primary amines before peptide conjugation. It appears that these amines impact the cellular uptake of the dendron. Dn6m and Dn6e both have 6 primary amines and significantly higher cellular uptake than Dn1 that only has 1 primary amine. Furthermore, Dn6e, which has all of the amines on the 5' terminal end of the dendron was taken up significantly more than the Dn6m, which had amines "buried" in the middle of the branches.

CD80 Costimulatory Marker Expression from Dendron-Peptide Conjugates

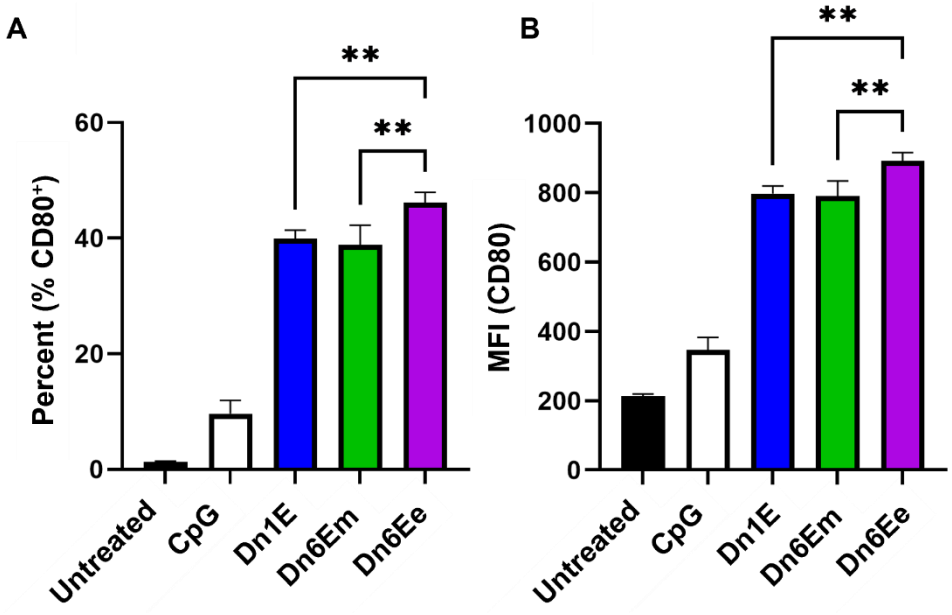

Figure S6. Cells treated with the peptide conjugates showed increases in CD80 expression frequency and amount. These trends match what was observed for the CD86 costimulatory marker in Figure 3E.

Uptake Pathway of Dendron-Peptide Conjugates

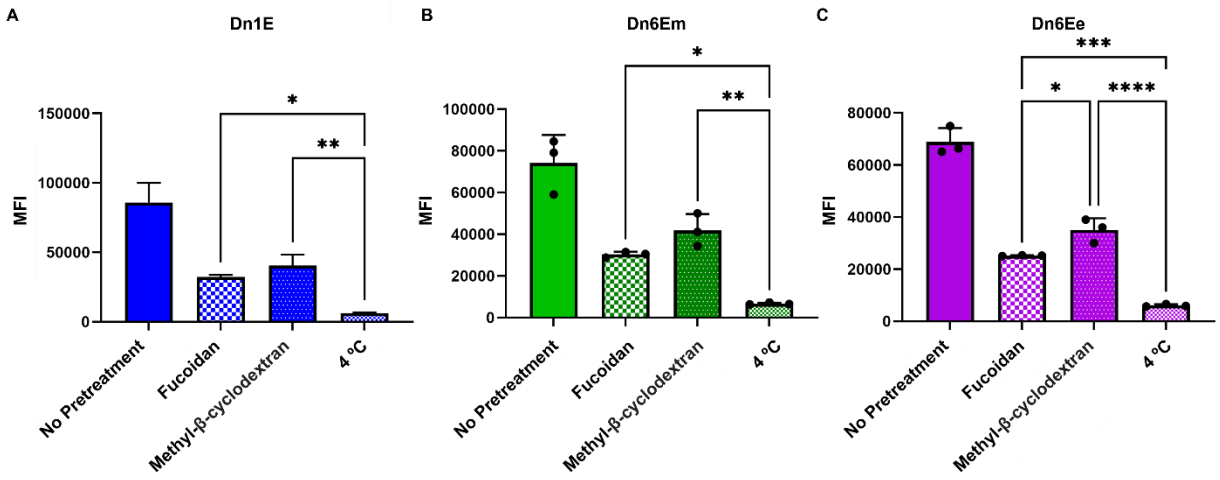

Figure S7. Cells were treated with peptide-dendron conjugates after pretreatment with either fucoidan (scavenger receptor A inhibitor) or methyl-beta-cyclodextran (depletes lipid raft and cholesterol) or after incubation at 4 °C (active transport inhibition). Dendrons are significantly taken up by active transport, which is mostly facilitated by scavenger receptor A and partly by hydrophobic-mediated processes.

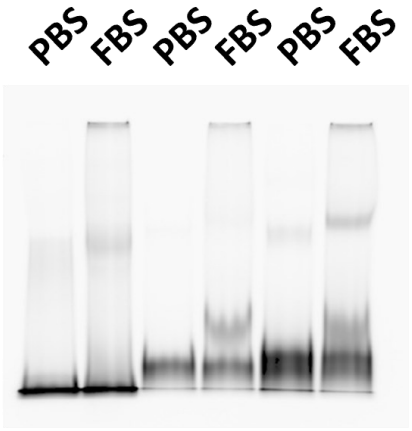

Figure S8. The effect of E6 peptide conjugation on the DNA dendron's protein corona was studied by incubating Dn1a, Dn1E, and Dn6Em at 18.45 μM in either FBS (PBS, 10% FBS) or pure PBS at 37degre°C for one hour with shaking. At the end of the one-hour incubation, sample corresponding to 0.03 OD (~0.112 nmole) from each reaction was loaded on a 10% native PAGE gel and run at a constant voltage of 100 volts for one hour. Upon completion, images were obtained using the ChemiDoc Gel Scanner (BioRad) with the cyanine 3 filter.

In Vivo Properties of DNA Dendron Vaccines

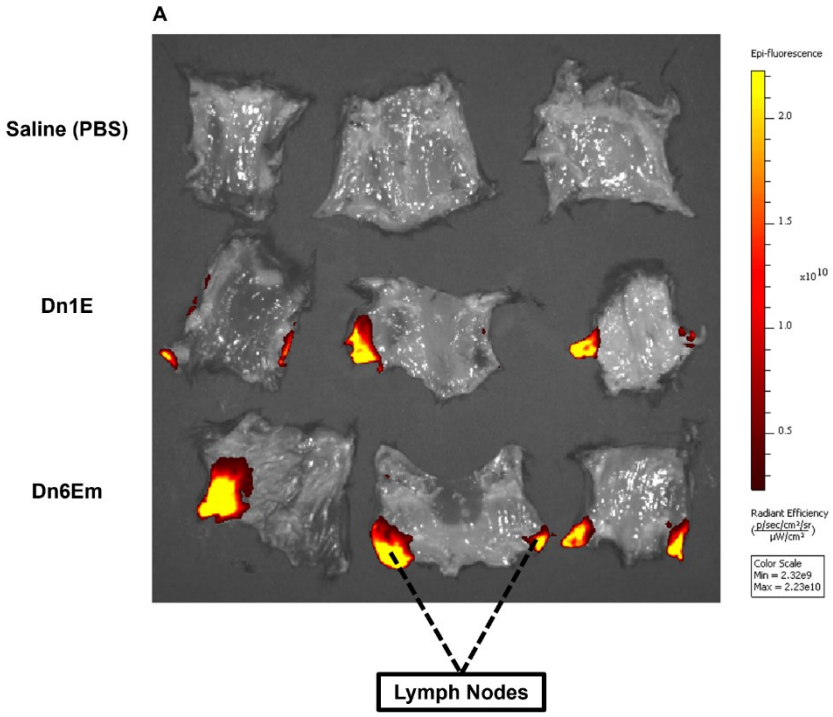

Figure S9. Female C57BL/6 mice (8-12 weeks old) were administered a single subcutaneous injection into the abdomen. The treatment dose was maintained at 6 nmol by Cy3 and dendron concentration. After 4 h, mice were euthanized, and the skin containing the lymph nodes was resected. Fluorescence was assessed using an IVIS 200 Spectrum (PerkinElmer) *in vivo* imaging system with a narrow band excitation of 535 nm and emission of 580 nm. Quantitative analysis was performed using Living Image software. The raw data presented here show that the Dn6Em vaccine is taken up by the lymph nodes more than the Dn1E vaccine.

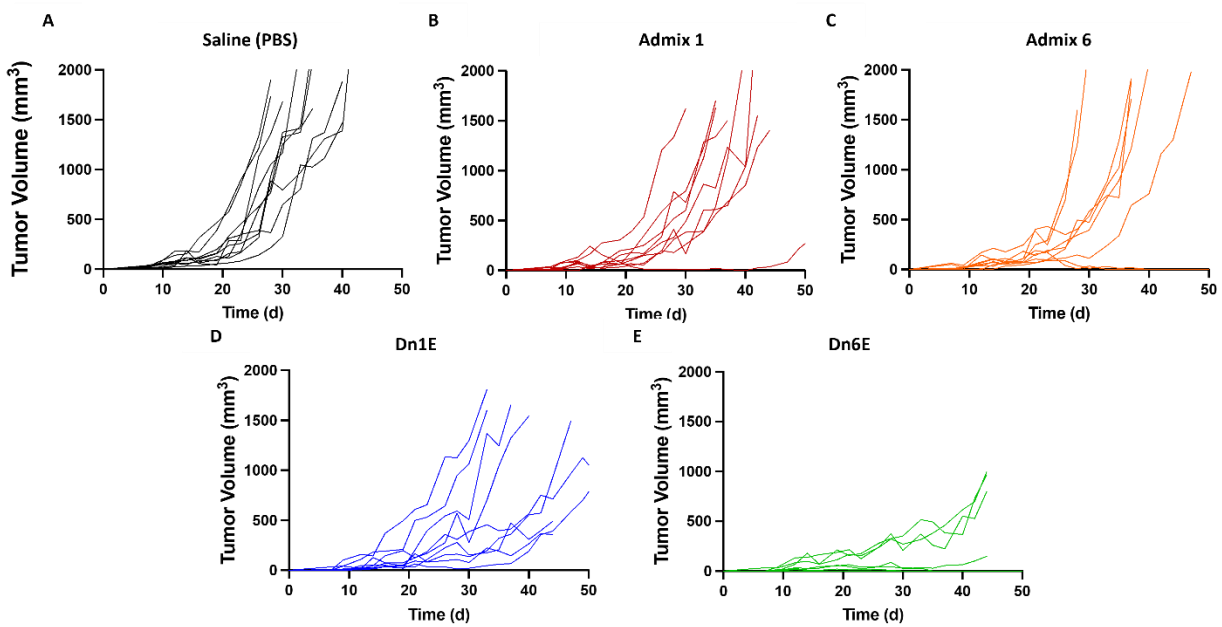

Figure S10. Female C57BL/6 mice aged 8-12 weeks (Jackson Laboratory) were inoculated with 2 x 10^5 TC-1 tumor cells subcutaneously into the right flank, and they were allowed to grow to ~50 mm^3 (7 days) prior to treatment. Treatments were administered at a dose of 60 μM in 100 μL volume by subcutaneous injection into the abdomen once per week, following the schedule provided. Tumor growth was measured every 2-3 days, and the volume was calculated using the following equation: tumor volume = length × $width^2$ × 0.5. Animals were euthanized when tumor volumes reached 1,500 mm^3 or when animal health necessitated sacrifice due to humane reasons. The spider plots of the individual mice in each group are presented.

Experimental Gating Strategies

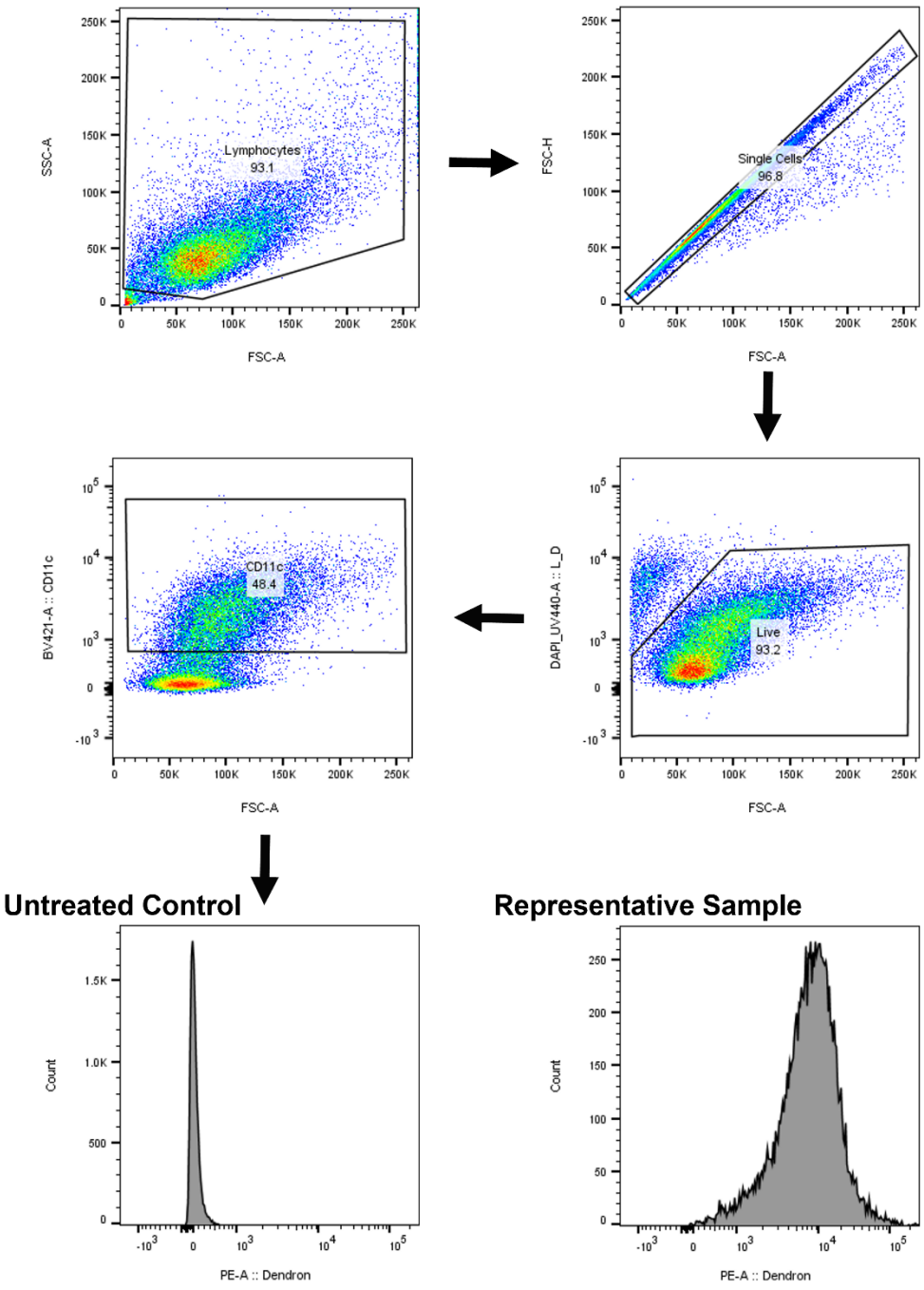

Figure S11. Gating strategy for Figure 1B and 1C.

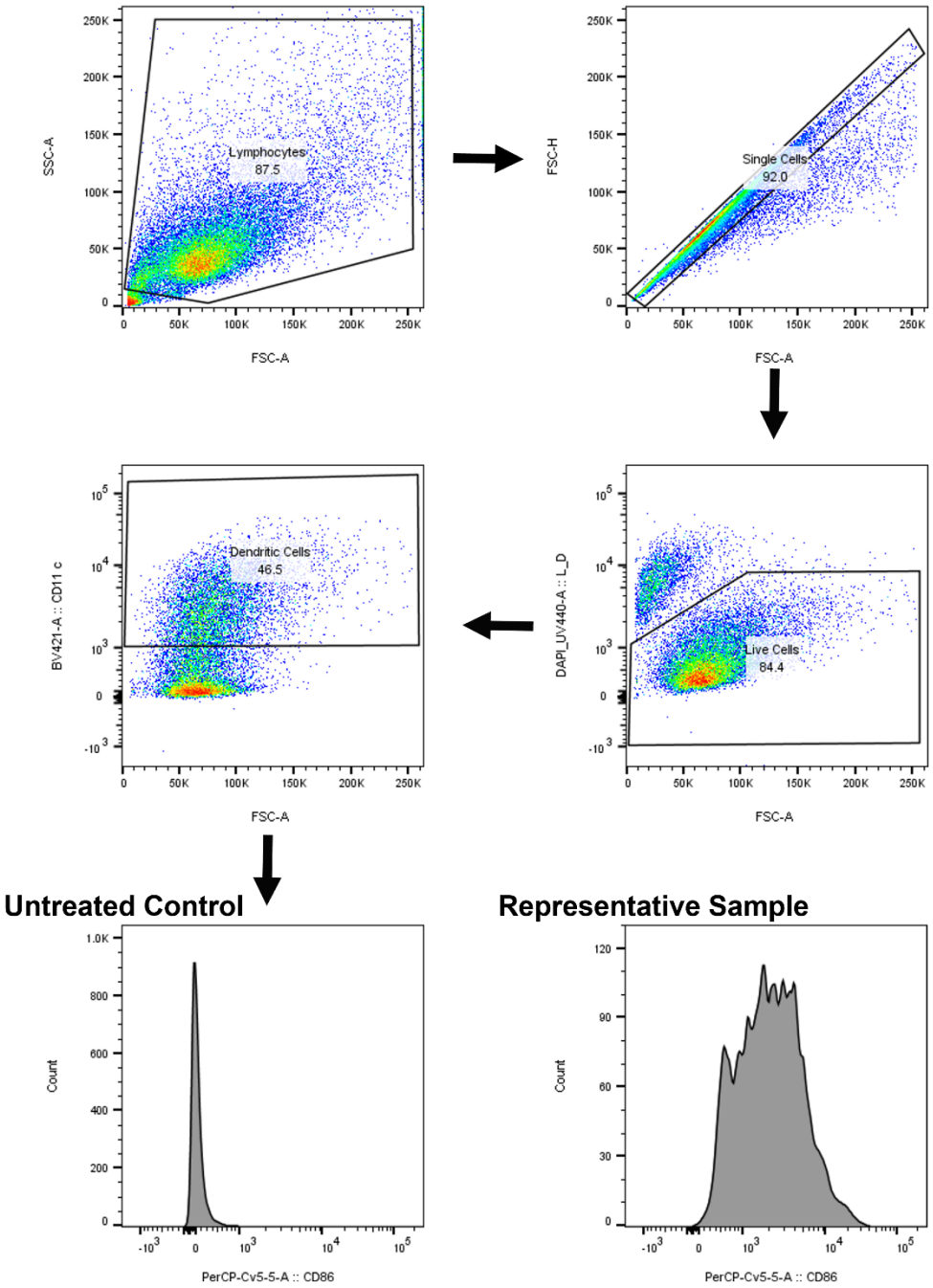

Figure S12. Gating strategy for Figures 2A, 2B, 3D, and 3E**.**

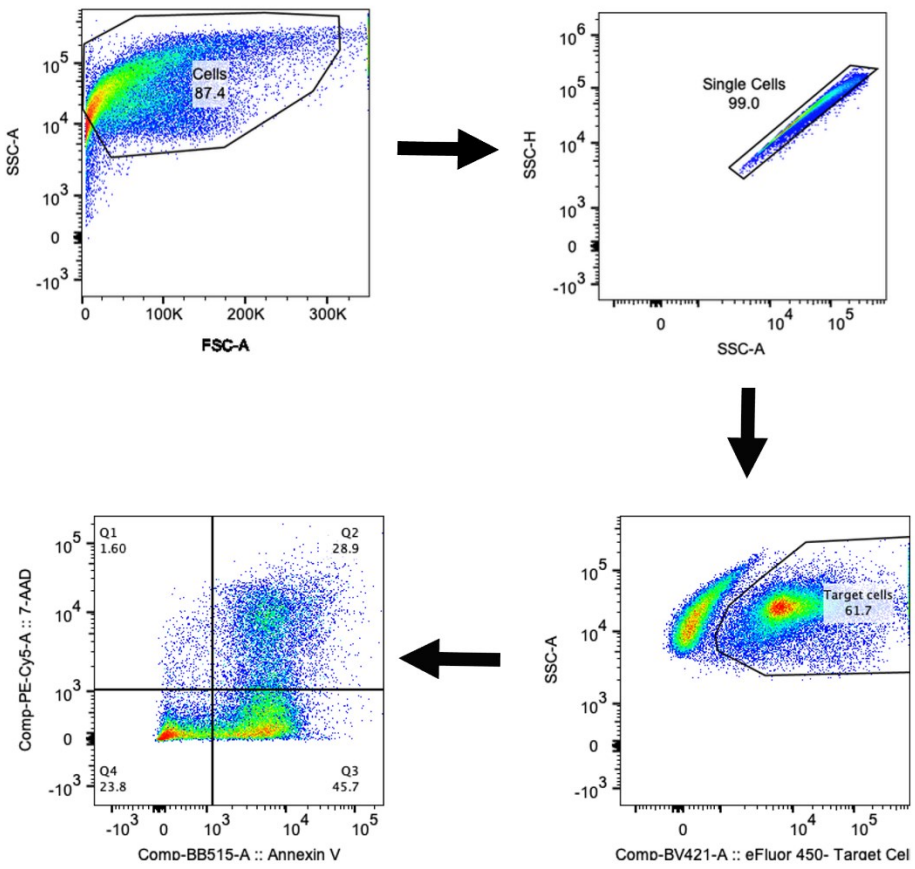

Figure S13. Gating strategy for Figure 4A.